UNIVERSIDAD NACIONAL DE COLOMBIA
SEDE MEDELLÍN
FACULTAD DE MINAS

DYNA
http://dyna.medellin.unal.edu.co/

Identification of ^{90}Sr and ^{204}Tl beta radiation sources by energy distribution with a 3GEM detector

Freddy Fuentes [a] & Rafael M. Gutiérrez [a, b]

[a] *Centro de investigaciones en Ciencias Básicas y Aplicadas, Universidad Antonio Nariño, Bogotá, Colombia, frefuentes@uan.edu.co, rafael.gutierrez@uan.edu.co*
[b] *Science Division, New York University Abu Dhabi, Abu Dhabi, United Arab Emirates, rmg2165@nyu.edu*

Received: January 15th, 2020. Received in revised version: September 22th, 2020. Accepted: October 1st, 2020

Abstract
This paper presents the performance of a 3GEM in terms of identification of high and low beta energy radiation sources through the energy distribution of the main beta radiation sources used for industrial application ^{90}Sr and ^{204}Tl. We compare the beta radiation theoretical energy loss into the drift zone with experimental energy distribution at different 3GEM voltages. The experimental results show that the Most Probable Value (MPV) of the fitted Landau distribution obtained from ^{90}Sr and ^{204}Tl obtained a degree of error lower than 14% in comparison to the theoretical calculation. Additionally, high energy beta radiation source (^{90}Sr) is identified in comparison to low energy (^{204}Tl) - taking into account the MPV and sigma values from the fitted Landau distribution. These results are essential to design and implement a new application that utilizes the performance and special characteristics of the 3GEM for beta radiation detection and identification.

Keywords: micro pattern gas detector; gas electron multiplier; Beta-radiation; energy distribution.

Identificación de fuentes de radiación beta 90Sr y 204Tl mediante distribución de energía con un detector 3GEM

Resumen
Este artículo presenta el rendimiento de un 3GEM en términos de identificación de fuentes de radiación beta de alta y baja energía utilizando la distribución de energía de las principales fuentes de radiación utilizadas para aplicaciones industriales: ^{90}Sr y ^{204}Tl. Comparamos la pérdida de energía de la radiación beta dentro de la zona de deriva respecto a datos experimentales a diferentes voltajes del 3GEM. Encontramos que el valor más probable (MPV) de la distribución Landau ajustada para ^{90}Sr y ^{204}Tl tuvo un error menor en un 14% en comparación con los cálculos teóricos. Además, se identifica la fuente de radiación beta de alta energía (^{90}Sr) en comparación con baja energía (^{204}Tl), teniendo en cuenta los valores de MPV y valor sigma de la distribución Landau ajustada. Estos resultados son esenciales para diseñar e implementar una nueva aplicación que explote el rendimiento y las características especiales del 3GEM para la detección e identificación de radiación beta.

Palabras clave: micro pattern gas detector; gas electron multiplier; radiación Beta; distribución energética.

1. Introduction

Geiger gaseous detectors have been an effective choice for applications using beta radiation sources, such as dosimetry [1,2] and thickness measurement [3-5]. Although this detector has a detection efficiency of up to 98% and a low cost, the Geiger detector is limited by the counting radiation process (the detector loses the information of the energy loss generated by the gas ionization). Studies using energy distribution analysis with scintillators and semiconductor detectors [6,7] have developed new algorithms for thickness measurement through radiation transmission with beta sources. Using the energy distribution analysis and identification of the beta radiation sources, new methods to improve the instrumentation accuracy and low level of uncertainty have been developed (+/-2mg/cm^2 for

How to cite: Fuentes, F. and Gutiérrez, R.M, Identification of ^{90}Sr and ^{204}Tl beta radiation sources by energy distribution with a 3GEM detector. DYNA, 87(215), pp. 174-179, October - December, 2020.

polyethylene absorber) [6]. However, a study of the identification of beta radiation sources using energy distribution with the latest gaseous detector technology has not yet been carried out. Gaseous detectors evolved to the Micro Pattern Gas Detectors (MPGDs). The MPGDs enhance all the characteristics of previous Geiger and proportional gaseous detectors in terms of detection capacity, energy, spatial and temporal resolution. The MPGDs have evolved mostly due to the interdisciplinary efforts of the CERN RD-51 collaboration program that is in charge of the Gaseous Detector Development (GDD) [8] - with the participation of many institutions from many countries around the world as well.

One of the MPGDs classes is the Gas Electron Multiplier (GEM). The GEM detector is a sealed chamber filled with some gases (normally, a mix of a noble and a quencher gas) composed of a drift (cathode), one or more GEM-foils (Three GEM-foils in our set-up), and a multichannel readout board (anode). The standard GEM-foil is a conductor-isolator-conductor layer with a pattern of triangular holes of 70µm in diameter and 140µm in pitch. The connection of the upper and bottom copper layers of the GEM-foil, with a differential voltage, creates a strong electric field through the holes. When a photon or charged particle ionizes the gases in the drift zone (Ed), an ion-electron pair is created. The electrons then must pass through the holes of the GEM-foil to reach the anode, and the ions travel in the opposite direction towards the cathode. As a result, when the electrons cross the high electric fields in the holes of the GEM-foil, an avalanche is generated that is proportional to the number of primary electrons produced in the drift zone [9-11].

For charged particles, the GEM has reached detection efficiencies greater than 95% when the effective gain of the detector is of order of 10^4, with an energy resolution between 15% and 25% [12,13]. These characteristics make the GEM detector an effective candidate for applications involving the beta sources previously mentioned in which the detection rate capability, temporal resolution, energy resolution, and detection efficiency are crucial. Most of the GEM studies demonstrate effective detector performance with photons generated by ^{55}Fe source for different applications [14]. Nevertheless, there is not enough information for the GEM performance in terms of energy loss in the drift zone, energy distribution, and possible identification of the main beta sources used in industrial applications.

In this work, all the features of experimentation set-up are described in Section 2. Section 3 shows the theoretical energy loss into the drift zone of the 3GEM of the beta sources used. The detector experimentation results in energy distribution were compared to the theoretical results obtained from ^{90}Sr and ^{204}Tl beta sources. Additionally, Section 3 shows the identification of ^{90}Sr and ^{204}Tl beta sources by energy distribution analysis. Finally, the conclusion of the 3GEM performance with beta radiation sources are discussed in Section 4.

2. 3GEM Assembly and experiment description

The parts and assembly of the 3GEM are presented in Fig.1. The parts are: the multichannel read-out board that is connected to the electronics and also serves as the detector support; the external frame with upper and lower O-rings for the detector tightness; the gas box cover to seal the top of the detector; a thin window made of mylar of 18.2mg/cm^2 to make the radiation lose the minimum amount of energy when it is passed through; the drift and the three GEM-foils in a cascade of 10x10cm^2 of area. The measurement of the gaps are: 3mm for the first ionization in the drift zone (Ed) and 2mm for the transfer zones one (Et1), two (Et2), and three (Et3).

All the detector components were assembled in the Detectors Laboratory at Universidad Antonio Nariño in a clean room (ISO 5) to guarantee an environment without dust. We acquired the GEM-foils from CERN. They were tested at 500V (with currents always below 3nA) to burn any possible microparticle inside the holes [12,15].

Once the detector was assembled, the set-up and connection of the different components are shown in Fig. 2. For the source voltage, we used a high voltage source CAEN NDT1470. The voltage distribution for the drift and the three GEM-foils was made with a voltage divisor. The voltage percentage for the first GEM-foil was 10%, 9.12% for the second, and 8.0% for the third GEM-foil. The voltage distribution given to the drift zone (Ed) and the transfer zones (Et1, Et2, y Et3) was a voltage percentage of 18.22% for each.

The mixture of gases used was Ar/CO_2 with a ratio of 70/30% at atmospheric pressure and at 20°C of temperature. The flux of the gases was 2.0+/-0.5l/h controlled by two flowmeters located at the detector input and output. For the detector start-up, we fluxed the 3GEM for several hours with Ar/CO_2 to remove humidity. Subsequently, we increased the total 3GEM voltage slowly until reaching 4100V -limiting the current of the voltage source to 4µA, and verifying that no sparks were inside the detector.

A preamplifier and shaper (APIC) made at CERN was used for the amplification process. The APIC was designed with a charge sensitive pre-amplifier (CSA) and a shaper stage with 1µs of peak time. We tested the APIC response by using and changing the voltage of a square wave generator followed by a capacitor of 1pF to generate known charges in the input (simulating the detector response). The APIC output voltage had a linear behavior with respect to the charge applied at the input with a relationship of 3mV/10^{-15}C with σ = 5.6mV. This calibration ensured the positive performance of the electronic amplifier before testing it with the 3GEM. The APIC output was connected to a Lecroy WaveRunner 62Xi oscilloscope of 600MHz bandwidth. All the components previously mentioned are shown in Fig. 2.

The main 3GEM parameters were measured at different voltages. Table 1 shows the results of our standard 3GEM working between 3600V and 4100V in terms of effective gain, energy resolution and detection rate

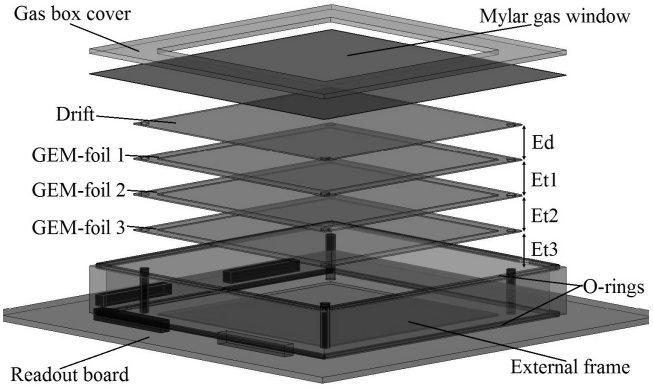

Figure 1. Parts of the standard 3GEM detector used at Antonio Nariño University.
Source: The Authors.

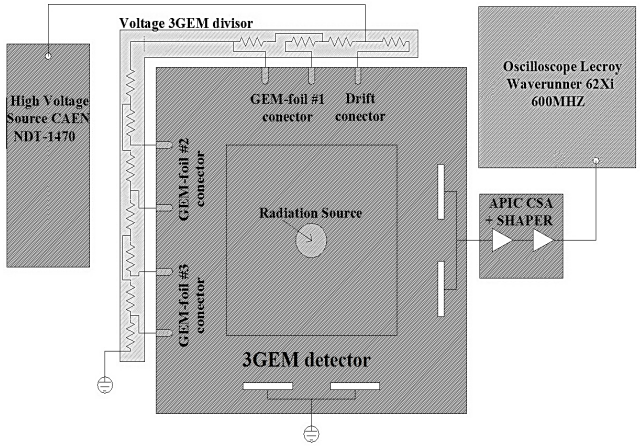

Figure 2. 3GEM detector Set-up consisting of a high voltage source, voltage divisor, 3GEM detector, radiation source, APIC and Oscilloscope.
Source: The Authors.

Table 1.

3GEM Voltage (V)	Effective gain	Energy resolution (%)	Efficiency in detection rate (%)
3600	330	35	72
3700	690	24	90
3800	1500	21	94
3900	2950	19	95
4000	6500	18	95
4100	9950	18	98

Source: The Authors

3. Detector response from beta radiation sources

This section is subdivided into the theoretical energy loss by beta radiation in the 3GEM drift zone; the comparison between the detector energy distribution and calculated energy loss; and the results of the fitted Landau distribution depending on the 3GEM total voltage for beta sources identification. All the results are from the ^{90}Sr, and ^{204}Tl radiation sources.

3.1. Theoretical energy loss

Due to the natural difference between X-ray and beta radiation, they have different interactions with matter. The X-ray photons interact by photoelectric, Compton and pair production. However, the beta electrons interact through ionization and Bremsstrahlung with the gas molecules of the gaseous detector. The energy loss of beta particles by unit length (dE/dx) is given by the Bethe-Bloch equation by eq. (1) [16,17]. In the case of a 3GEM, there is a trajectory of energy loss of about 3mm of length filled with Ar/CO_2 with a proportion of 70/30% in the drift zone (Ed).

$$-\frac{dE}{dx} = 4\pi {r_o}^2 \frac{mc^2}{\beta^2} NZ \left\{ \ln\left(\frac{\beta\gamma\sqrt{\gamma-1}\, mc^2}{I} \right) + \frac{1}{2\gamma^2}\left[\frac{(\gamma-1)^2}{8} + 1 - (\gamma^2 + 2\gamma - 1) ln2 \right] \right\} \quad (1)$$

In eq. (1): r_o is the electron radius, mc^2 is the rest energy of the electron, N is the number of atoms by cubic meter in the absorber material, Z is the atomic number of the absorber material, β is the relative phase velocity of the particle, and γ is the Lorentz factor [16]. However, this formula is applied to monoenergetic electrons and takes into account only the ionization effects. For non-monoenergetic beta radiation sources (such as ^{90}Sr and ^{204}Tl), it is necessary to obtain an approximation of the average energy of the electrons given by $E_{av} = E_{max}/3$ (E_{av} ^{90}Sr =760keV, E_{av} ^{204}Tl =254keV). The total energy loss is found by dE/dx total = $dE/dx_{ionization}$+ $dE/dx_{Bremsstrahlung}$, where an approximation of the energy loss by Bremsstrahlung is $dE/dx_{Bremsstrahlung} = Z*E_{av}/750MeV * dE/dx_{ionization}$ [16]. Fig. 3 shows the energy loss in MeV*cm^2/g for the E_{av} of the ^{90}Sr and ^{204}Tl beta sources in Argon (top) and in CO_2 (bottom).

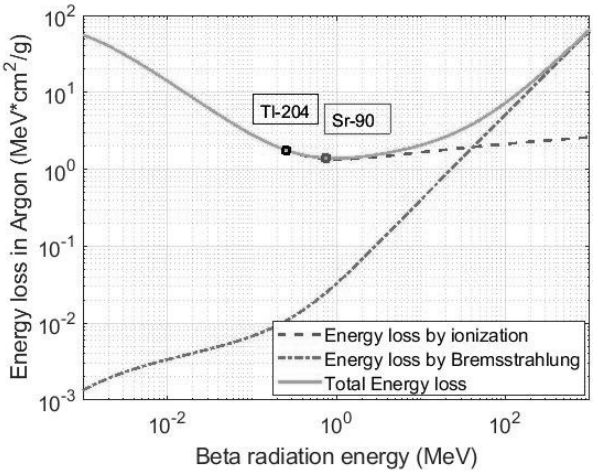

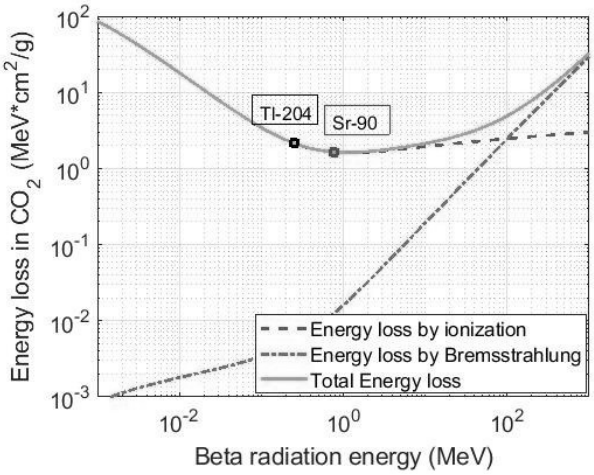

Figure 3. Total energy loss, energy loss by ionization, and energy loss by Bremsstrahlung in Argon (top) and CO_2 (bottom) gases calculated by eq. (1).
Source: The Authors.

Fig. 3 shows that energy loss by ionization is dominant and energy loss by Bremsstrahlung was negligible for the beta sources in both gases. The amount of energy loss calculated for the drift zone Ed (3mm) of the 3GEM detector with a mixture of Ar/CO_2 in a proportion of 70/30%, was 745eV for ^{90}Sr and 968eV for ^{204}Tl. It is notable that the higher a source energy (up to $E_{av} \sim 2MeV$), the less energy loss in the gases.

3.2. Experimental 3GEM energy distribution

The energy distribution generated by beta particles is shown by a Landau distribution in Fig. 4. The energy distribution shown is a Gaussian distribution at low energies but has a long tail towards high energies. This tail corresponds to the beta particles close interactions with the target nuclei [18,19]. We obtained the energy distribution from the peak voltage of the APIC output (taking into account the mentioned APIC output of $3mV/10^{-15}C$). Two parameters are fundamental for the Landau distribution: the Most Probable Value (MPV), that is the more frequent value of energy loss in the histogram (located on the peak Landau distribution), and the sigma value (σ). Fig. 4 shows the experimental energy spectrum taken from the 3GEM working with Ar/CO_2 in a proportion of 70/30% at 3700V, as well as the fitted Landau distribution. We checked that the fitted Landau distribution corresponded to the recorded data generated by the detector.

Fig. 5 shows the previous energy loss calculated (squares) in the drift zone (Ed) of the 3GEM from the beta radiation sources ^{90}Sr (0.745keV) and ^{204}Tl (0.968keV). It also shows the normalized fitted energy distribution obtained with the 3GEM detector for the beta sources as well as from the soft X-ray photons generated by a ^{55}Fe source. In the histogram, in order to pass from peak voltage to energy in the X-axis, it is necessary to introduce a knowing energy distribution, such as a ^{55}Fe source. The ^{55}Fe photons of the soft X-ray source transmit most of their energy through the photoelectric effect. From the ^{55}Fe energy spectrum in Fig. 5, the bigger peak corresponds to the detection of photons at 5.9keV and the second peak of 3.0keV to the Argon escape - with it being 15% of the main peak. After obtaining the ^{55}Fe energy distribution, it is possible to pass from peak voltage to energy in the X-axis as is seen in Fig.5.

Even when the average energy E_{av} from beta radiation sources is much higher than the ^{55}Fe source (E_{av} ^{90}Sr =760keV, E_{av} ^{204}Tl =254keV), the beta sources lose a minimum amount of energy by ionization into the drift zone of the 3GEM (1% for ^{90}Sr and 3.8% for ^{204}Tl). Fig. 5 shows that the beta radiation sources energy loss calculated (squares) is close to the MPV fitted Landau distribution obtained by the 3GEM. Additionally, Fig. 5 shows that the ^{90}Sr sigma of the fitted Landau distribution is sufficiently different to distinguish from ^{204}Tl (difference of 18%).

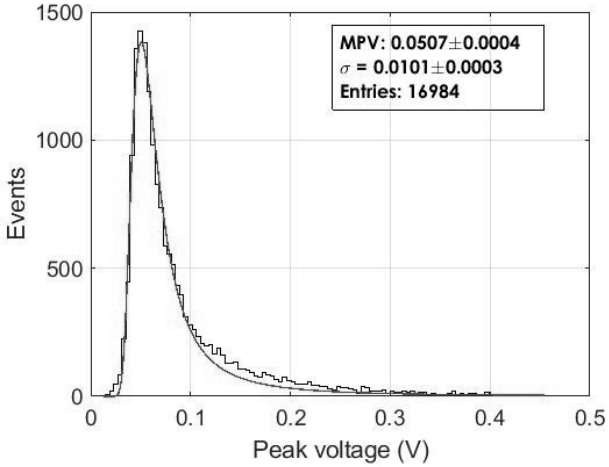

Figure 4. 3GEM energy distribution from ^{90}Sr with Ar/CO_2 in a proportion of 70/30% at 3700V, and the fitting Landau distribution.
Source: The Authors.

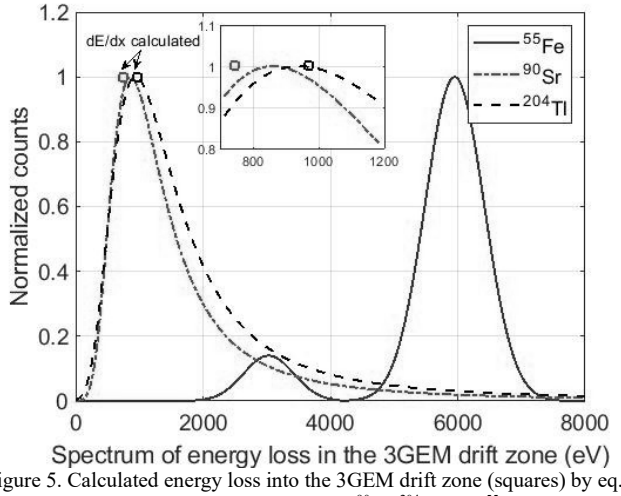

Figure 5. Calculated energy loss into the 3GEM drift zone (squares) by eq. (1) and fitted energy distribution from beta ^{90}Sr, ^{204}Tl, and ^{55}Fe radiation sources obtained by the 3GEM.
Source: The Authors.

Figs. 6, 7 show the MPV and sigma values from the fitted Landau distribution provided by the 3GEM detecting the beta sources used at different voltages. It is possible to see three main characteristics in the graph. When the 3GEM is working below 4000V, both fitted spectra are similar (MPV and sigma) and it is not possible to identify which distribution corresponds to its radiation source. At 4000V, it is possible to differentiate the MPV and the sigma value from the fitted beta radiation sources. However, the error bars, either the MPV or sigma ones, make it possible to confuse the identification of each beta source. For 4100V, it is clear to identify each beta radiation source through the fitted distribution due to there being enough difference in the MPV and sigma values. The 3GEM high effective gain and energy resolution working at 4100V (showed in Table 1) clarify significantly the fitted energy spectrum beta radiation sources of high energy (^{90}Sr) in comparison to low energy (^{204}Tl) - taking into consideration the MPV and sigma values of the fitted Landau distribution

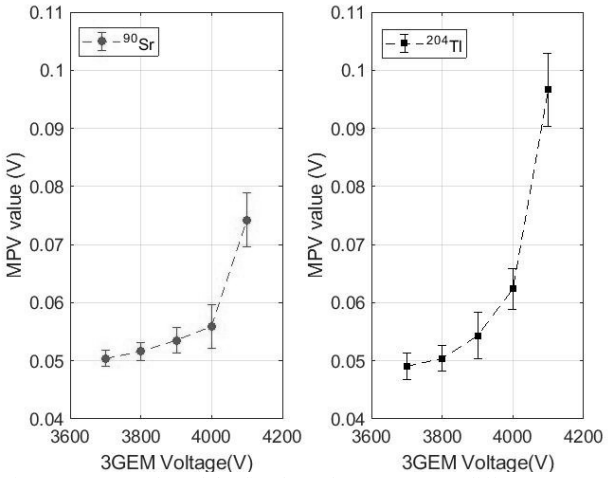

Figure 6. MPV value of the fitted Landau spectrum at different 3GEM voltages from ^{90}Sr and ^{204}Tl beta sources.
Source: The Authors.

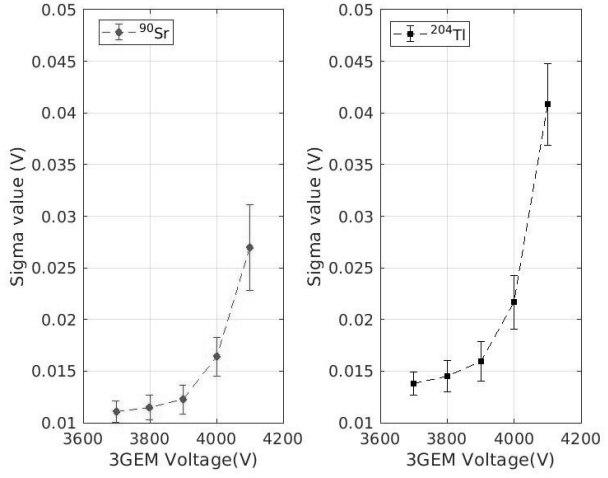

Figure 7. Sigma value of the fitted Landau spectrum at different 3GEM voltages from ^{90}Sr and ^{204}Tl beta sources.
Source: The Authors.

4. Conclusions

The standard 3GEM detector demonstrates that through energy distribution, it is possible to differentiate the main beta sources used in the industry for applications such as tracking, thickness measurement, and dosimetry. We demonstrated that although the standard 3GEM has a minimum volume of gases in the drift zone (which makes minimal differences on the energy loss between different beta radiation energies), the calculated energy loss by Bethe-Bloch formula, and the experimental energy loss results were close (errors of 12.9% from ^{90}Sr, and 3.3% from ^{204}Tl). Additionally, with an energy resolution of 19%, measured at 4100V Ar/CO_2, in proportion of 70/30%, it was possible to differentiate the energy distribution of high energy (^{90}Sr) and the low energy (^{204}Tl) beta radiation sources by the MPV (for ^{90}Sr = 74.2mV (+/- 6.3%), and for ^{204}Tl = 96.6mV (+/- 6.5%)) and sigma values (^{90}Sr σ = 26.99mV (+/- 15.4%), and from ^{204}Tlσ = 40.84mV (+/- 9.7%)) of the fitted Landau distribution. The characteristics measured previously with the 3GEM confirm that the detector has optimum performance in applications where the energy distribution analysis is essential in terms of accuracy and precision of the application. We will work in further studies on increasing the drift zone Ed (for a higher energy loss dE/dx) as well as changing the gases mixture and pressure in order to strengthen the 3GEM performance in terms of beta source identification.

Acknowledgments

The authors acknowledge the CERN Gaseous Detector Development (GDD) group for the capacitation in the building and start-up of the 3GEM and to Colciencias for the financial support with laboratory equipment and doctorate studies through call # 727.

References

[1] Soares, C.G., Vynckier, S., Järvinen, H., Cross, W.G. Sipilä, P., Flühs, D., Schaeken, B., Mourtada, F.A., Bass, G.A. and Williams, T.T., Dosimetry of beta-ray ophthalmic applicators: Comparison of different measurement methods, Medical Physics, 28(7), pp. 1373-1384, 2001. DOI: 10.1118/1.1376441

[2] Hine, G.J., Radiation dosimetry. Academic Press, 2013.

[3] Zipf, M.E., Radiation transmission-based thickness measurement systems - Theory and applications to flat rolled strip products, in: Advances in measurement systems, Sharma, M.Kr., Ed., 2010, pp. 105-160. DOI: 10.5772/8729

[4] Şen, M. and Çalik, A.E., Calculation of half-value thickness for aluminum absorbers by means of fractional calculus, Annals of Nuclear Energy, 63, 2014, pp. 46-50. 2014. DOI: 10.1016/j.anucene.2013.07.023

[5] Brasunas, J.C., Cushman, G.M. and Lakew, B., Thickness Measurement. CRC Press, 1999.

[6] Yalcin, S., Gurler, O., Gundogdu, O. and Bradley, D.A., A practical method for in-situ thickness determination using energy distribution of beta particles, Applied Radiation and Isotopes, 70(1), pp. 128-132, 2012. DOI: 10.1016/j.apradiso.2011.08.001

[7] Grozev, P.A., Vapirev, E.I. and Botsova, L.I. Energy distribution of beta-particles transmitted through an absorber, Applied Radiation and Isotopes, 43(3), pp 383-387, 1992. DOI: 10.1016/0883-2889(92)90110-Z

[8] Titov M. and Ropelewski, L., Micro-pattern gaseous detector technologies and RD51 collaboration, Modern Physics Letters A, 28(13), pp. 1340022, 2013. DOI: 10.1142/S0217732313400221
[9] Sauli, F., GEM: A new concept for electron amplification in gas detectors, Nuclear Instruments Methods in Physics Section A, 386 (2-3), pp. 531-534, 1997. DOI: 10.1016/S0168-9002(96)01172-2
[10] Bouclier, R., Dominik, W., Hoch, M., Labbe, J.-C., Million, G., Ropelewski, L., Sauli, F., Sharma, A. and Manzin, G., New observations with the gas electron multiplier (GEM), Nuclear Instruments Methods in Physics Section A, 396 (1-2), pp. 50-66, 1997. DOI: 10.1016/S0168-9002(97)00648-7
[11] Bellazzini, R., Brez, A., Gariano, G., Latronico, L., Lumb, N., Spandre, G., Massai, M.M., Raffo, R. and Spezziga, M.A., What is the real gas gain of a standard GEM?, Nuclear Instruments Methods in Physics Section A, 419 (2-3), pp. 429-437, 1998. DOI: 10.1016/S0168-9002(98)00856-0
[12] Altunbas, C., Capéans, M., Dehmelt, K., Ehlers, J., Friedrich, J., Konorov, I., Gandi, A., Kappler, S., Ketzer, B., De Oliveira, R., Paul, S., Placci, A., Ropelewski, L., Sauli, F., Simon, F. and van Stenis, M., Construction, test and commissioning of the triple-gem tracking detector for compass, Nuclear Instruments Methods in Physics Section A, 490 (1-2), pp. 177-203, 2002. DOI: 10.1016/S0168-9002(02)00910-5
[13] Sauli, F., The Gas Electron Multiplier (GEM): operating principles and applications, Nuclear Instruments Methods in Physics Section A, 805, pp. 2-24, 2016. DOI: 10.1016/j.nima.2015.07.060
[14] Sauli, F., Radiation imaging with gaseous detectors, Nuclear Instruments Methods in Physics Section A, 878, pp. 1-9, 2018. DOI: 10.1016/j.nima.2017.01.056
[15] Ziegler, M., Development of a triple GEM detector for the LHCb experiment, PhD Dissertation, Faculty of Mathematics and Natural Sciences, University of Zurich, Zurich, 2002.
[16] L'Annunziata, M.F., Handbook of radioactivity analysis. Academic Press, 2012.
[17] Leroy, C. and Rancoita, P.-G., Principles of Radiation interaction in matter and detection. World Scientific, 2015.
[18] Sauli, F., Principles of operation of multiwire proportional and drift chambers, Experimental Techniques in High-Energy Nuclear and Particle Physics, pp. 79-188, 1991. DOI: 10.1142/9789814355988_0002
[19] Rolandi, L., Riegler, W. and Blum, W., Particle detection with drift chambers, Springer Verlag, 1993.

F. Fuentes, received a BSc. Eng. in Electronic Engineering in 2013, Sp. in Industrial Automation in 2015, and PhD. in Applied Science in 2020. He worked for manufacturing companies within the automation and maintenance sector for ten years. His research interests include: simulation, automation and control, instrumentation, radiation detectors, and electronics for radiation detectors.
ORCID: 0000-0003-4382-853X

R.M. Gutierrez, received a BSc. in Physics in 1989, a MSc. in Physics of Condensed Matter in 1993, and a PhD. in Physics Applied Science in 1997. He worked at Colciencias as Director of Scientific and Technological Development Programs. He also was the Applied Science Doctorate director for seven years. He is currently working as professor at the New York University in Abu Dhabi.
ORCID: 0000-0001-5734-6174